Lecture 4: Dark Matter Searches at e^+e^- Colliders

Zhao-Huan Yu（余钊焕）

ARC Centre of Excellence for Particle Physics at the Terascale,
School of Physics, the University of Melbourne
http://yzhxxzxy.github.io

Frontiers in Dark Matter, Neutrinos, and Particle Physics
Theoretical Physics Summer School

Sun Yat-Sen University, Guangzhou
July 27-28, 2017

Monophoton Searches at e^+e^- Colliders

PHYSICAL REVIEW D **88,** 075015 (2013)

Detecting interactions between dark matter and photons at high energy e^+e^- colliders

Zhao-Huan Yu,[1] Qi-Shu Yan,[2,3] and Peng-Fei Yin[1]

[1]*Key Laboratory of Particle Astrophysics, Institute of High Energy Physics, Chinese Academy of Sciences, Beijing 100049, China*
[2]*College of Physics Sciences, University of Chinese Academy of Sciences, Beijing 100049, China*
[3]*Center for High Energy Physics, Peking University, Beijing 100871, China*
(Received 30 July 2013; published 24 October 2013)

We investigate the sensitivity to the effective operators describing interactions between dark matter particles and photons at future high energy e^+e^- colliders via the $\gamma + \not{E}$ channel. Such operators could be useful to interpret the potential gamma-ray line signature observed by the Fermi-LAT. We find that these operators can be further tested at e^+e^- colliders by using either unpolarized or polarized beams. We also derive a general unitarity condition for $2 \to n$ processes and apply it to the dark matter production process $e^+e^- \to \chi\chi\gamma$.

DOI: 10.1103/PhysRevD.88.075015 PACS numbers: 95.35.+d, 12.60.−i, 13.66.Hk

[arXiv:1307.5740, PRD]

γ-ray emission from DM: continuous spectrum

Dark matter (DM, χ) pair annihilation or decay into

e^+e^-, $\mu^+\mu^-$, $\tau^+\tau^-$, $q\bar{q}$, W^+W^-, Z^0Z^0, h^0h^0

$\Downarrow$

Gamma-ray emission from final state radiation or decay

Cut-off energy: m_χ for DM annihilation, $m_\chi/2$ for DM decay

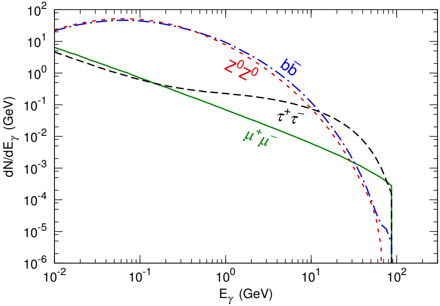

γ-ray emission from DM: continuous spectrum

Dark matter (DM, χ) pair annihilation or decay into

$$e^+e^-,\ \mu^+\mu^-,\ \tau^+\tau^-,\ q\bar{q},\ W^+W^-,\ Z^0Z^0,\ h^0h^0$$

$$\Downarrow$$

Gamma-ray emission from final state radiation or decay

Cut-off energy: m_χ for DM annihilation, $m_\chi/2$ for DM decay

Searching for DM signature in DM-dominant regions:

Galactic center

Galactic halo

dwarf spheroidal galaxies

clusters of galaxies

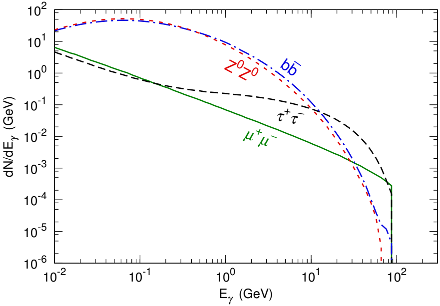

γ-ray Emission from DM: Line Spectrum

In general, DM particles (χ) should not have electric charge
and not directly couple to photons

$\Downarrow$

DM particles may couple to photons via high order loop diagrams

(highly suppressed, the branching fraction may be only $\sim 10^{-4} - 10^{-1}$)

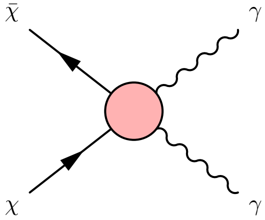

γ-ray Emission from DM: Line Spectrum

In general, DM particles (χ) should not have electric charge and not directly couple to photons

$\Downarrow$

DM particles may couple to photons via high order loop diagrams

(highly suppressed, the branching fraction may be only $\sim 10^{-4} - 10^{-1}$)

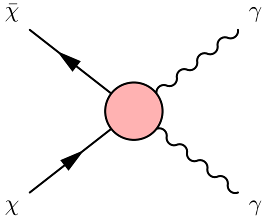

For **nonrelativistic** DM particles, the photons produced in $\chi\chi \to \gamma\gamma$ would be **mono-energetic**

$\Downarrow$

A γ-ray line at energy $\sim m_\chi$

(**"smoking gun"** for DM particles)

A γ-ray Line Signal from the Galactic Center Region?

Using the 3.7-year Fermi-LAT γ-ray data, several analyses showed that there might be evidence of **a monochromatic γ-ray line at energy** $\sim 130\,\mathrm{GeV}$, originating from the Galactic center region (about $3-4\sigma$).

It may be due to DM annihilation with $\langle\sigma_{\mathrm{ann}}v\rangle \sim 10^{-27}\,\mathrm{cm}^3\,\mathrm{s}^{-1}$.

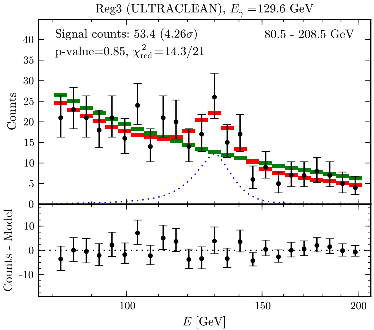

Weniger, 1204.2797

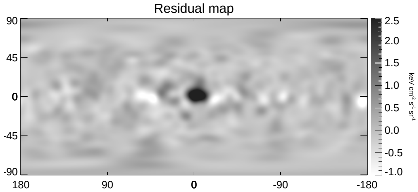

Su & Finkbeiner, 1206.1616

A γ-ray Line Signal from the Galactic Center Region?

The Fermi-LAT Collaboration has released its official spectral line search in the energy range $5-300\,\text{GeV}$ using 3.7 years of data.

They **did not find any globally significant lines** and set 95% CL upper limits for DM annihilation cross sections.

Their most significant fit occurred at $E_\gamma = 133\,\text{GeV}$ and had **a local significance of 3.3σ**, which translates to a global significance of 1.6σ.

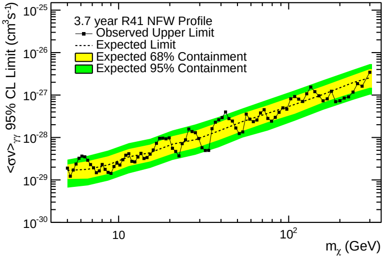

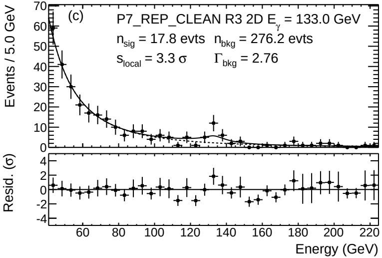

Fermi-LAT Collaboration, 1305.5597

DM-photon Interaction at e^+e^- Colliders

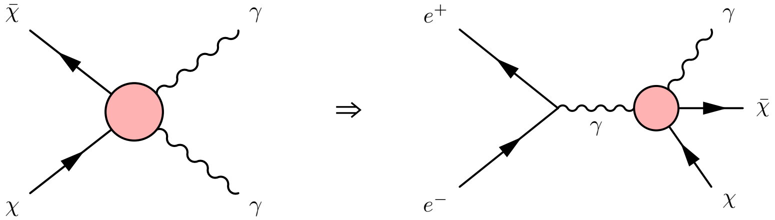

The coupling between DM particles and photons that induce the annihilation process $\chi\chi \to \gamma\gamma$ can also lead to the process $e^+e^- \to \chi\chi\gamma$. Therefore, the possible γ-ray line signal observed by Fermi-LAT may be tested at future TeV-scale e^+e^- colliders.

DM particles escape from the detector

$\Downarrow$

Signature: a **monophoton** associating with missing energy $(\gamma + \not{E})$

Effective Operator Approach

If DM particles couple to photons via exchanging some mediators which are **sufficiently heavy**, the DM-photon coupling can be approximately described by **effective contact operators**.

For Dirac fermionic DM, consider $\mathcal{O}_F = \frac{1}{\Lambda^3}\bar{\chi} i\gamma_5 \chi F_{\mu\nu}\tilde{F}^{\mu\nu}$**:**

$$\langle \sigma_{\mathrm{ann}} v\rangle_{\chi\bar{\chi}\to 2\gamma} \simeq \frac{4m_\chi^4}{\pi\Lambda^6}, \qquad \sigma(e^+e^- \to \chi\bar{\chi}\gamma) \sim \frac{s^2}{\Lambda^6}$$

Fermi γ-ray line signal $\Longleftrightarrow$ $m_\chi \simeq 130\,\mathrm{GeV},\ \Lambda \sim 1\,\mathrm{TeV}$

For complex scalar DM, consider $\mathcal{O}_S = \frac{1}{\Lambda^2}\chi^*\chi F_{\mu\nu}F^{\mu\nu}$**:**

$$\langle \sigma_{\mathrm{ann}} v\rangle_{\chi\chi^*\to 2\gamma} \simeq \frac{2m_\chi^2}{\pi\Lambda^4}, \qquad \sigma(e^+e^- \to \chi\chi^*\gamma) \sim \frac{s}{\Lambda^4}$$

Fermi γ-ray line signal $\Longleftrightarrow$ $m_\chi \simeq 130\,\mathrm{GeV},\ \Lambda \sim 3\,\mathrm{TeV}$

Simulation

In the $\gamma + \not{E}$ searching channel, the main background is $e^+e^- \to \nu\bar{\nu}\gamma$:

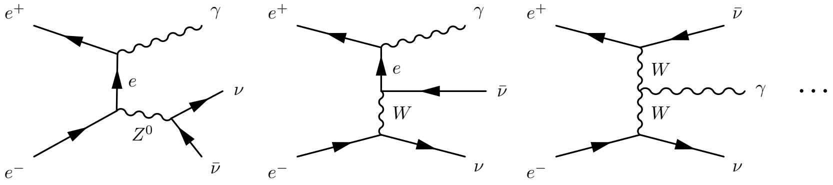

Minor backgrounds: $e^+e^- \to e^+e^-\gamma$, $e^+e^- \to \tau^+\tau^-\gamma$, $\cdots$

Simulation: `FeynRules` $\to$ `MadGraph 5` $\to$ `PGS 4`

ILD-like ECAL energy resolution: $\dfrac{\Delta E}{E} = \dfrac{16.6\%}{\sqrt{E/\text{GeV}}} \oplus 1.1\%$

Future e^+e^- colliders: $\sqrt{s} = 250\,\text{GeV}$ ("Higgs factory"), $\sqrt{s} = 500\,\text{GeV}$ (typical ILC), $\sqrt{s} = 1\,\text{TeV}$ (upgraded ILC & initial CLIC), $\sqrt{s} = 3\,\text{TeV}$ (ultimate CLIC)

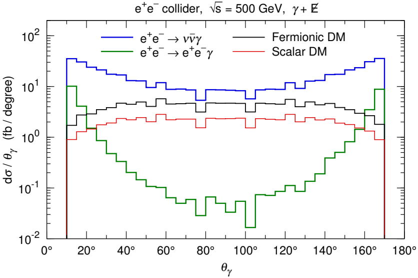

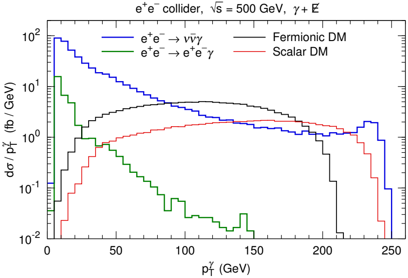

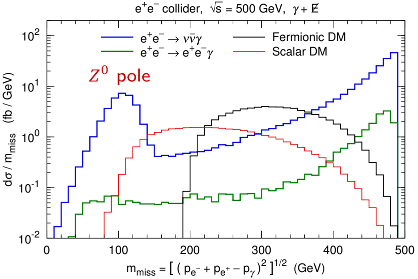

Cut 1 (pre-selection):

Require a photon with $E_\gamma > 10\,\text{GeV}$ and $10^\circ < \theta_\gamma < 170^\circ$

Veto any other particle

Benchmark point: $\Lambda = 200\,\text{GeV}$, $m_\chi = 100\,(50)\,\text{GeV}$ for fermionic (scalar) DM

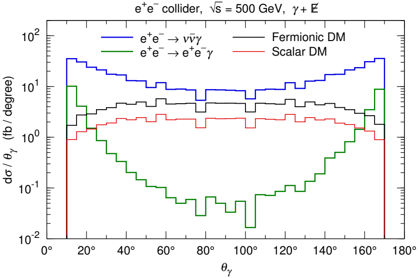

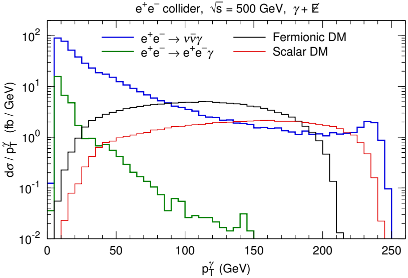

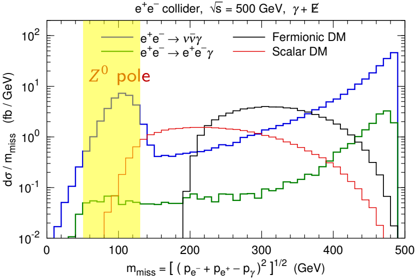

Cut 1 (pre-selection):
Require a photon with $E_\gamma > 10\,\text{GeV}$
and $10^\circ < \theta_\gamma < 170^\circ$
Veto any other particle

Cut 2: Veto $50\,\text{GeV} < m_{\text{miss}} < 130\,\text{GeV}$

Benchmark point: $\Lambda = 200\,\text{GeV}$, $m_\chi = 100\,(50)\,\text{GeV}$ for fermionic (scalar) DM

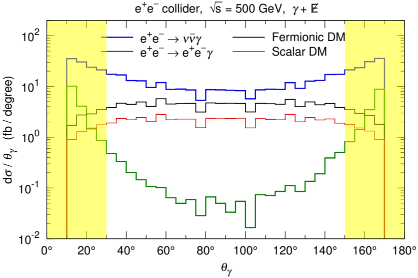

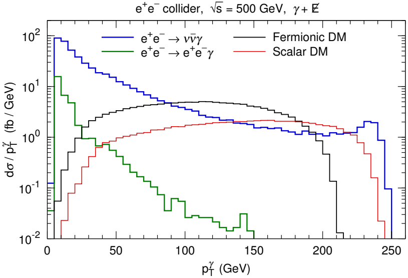

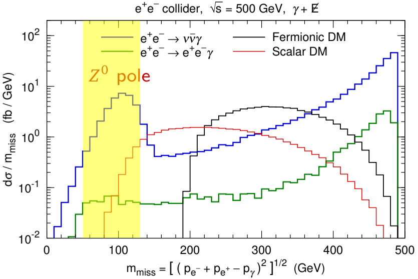

Cut 1 (pre-selection):
Require a photon with $E_\gamma > 10\,\text{GeV}$
and $10^\circ < \theta_\gamma < 170^\circ$
Veto any other particle

Cut 2: Veto $50\,\text{GeV} < m_{\text{miss}} < 130\,\text{GeV}$

Cut 3: Require $30^\circ < \theta_\gamma < 150^\circ$

Benchmark point: $\Lambda = 200\,\text{GeV}$, $m_\chi = 100\,(50)\,\text{GeV}$ for fermionic (scalar) DM

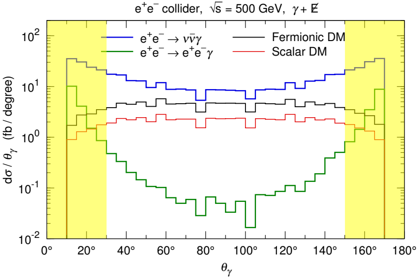

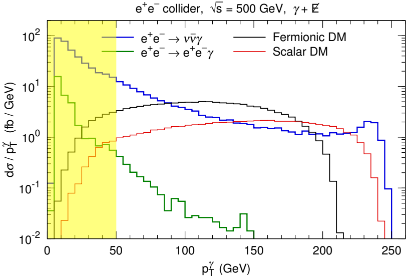

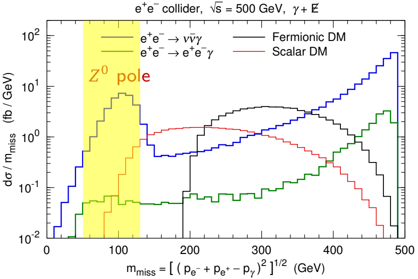

Cut 1 (pre-selection):
Require a photon with $E_\gamma > 10\,\mathrm{GeV}$
and $10^\circ < \theta_\gamma < 170^\circ$
Veto any other particle

Cut 2: Veto $50\,\mathrm{GeV} < m_{\mathrm{miss}} < 130\,\mathrm{GeV}$

Cut 3: Require $30^\circ < \theta_\gamma < 150^\circ$

Cut 4: Require $p_{\mathrm{T}}^{\gamma} > \sqrt{s}/10$

Benchmark point: $\Lambda = 200\,\mathrm{GeV}$, $m_\chi = 100\,(50)\,\mathrm{GeV}$ for fermionic (scalar) DM

Cut Flow

Cross sections and signal significances after each cut

	$\nu\bar{\nu}\gamma$	$e^+e^-\gamma$	Fermionic DM		Scalar DM	
	σ (fb)	σ (fb)	σ (fb)	$S/\sqrt{B}$	σ (fb)	$S/\sqrt{B}$
Cut 1	**2415.2**	**173.0**	646.8	12.7	321.4	6.3
Cut 2	2102.5	168.6	646.8	13.6	308.2	6.5
Cut 3	1161.1	16.8	538.0	15.7	255.9	7.5
Cut 4	**254.5**	**1.9**	520.7	32.5	253.9	15.8

Benchmark point: $\Lambda = 200\,\text{GeV}$, $m_\chi = 100\,(50)\,\text{GeV}$ for fermionic (scalar) DM

Most of the signal events remain

$e^+e^- \to \nu\bar{\nu}\gamma$ background: reduced by almost **an order of magnitude**

$e^+e^- \to e^+e^-\gamma$ background: only **one percent** survives

$(\sqrt{s} = 500\,\text{GeV},\ 1\,\text{fb}^{-1})$

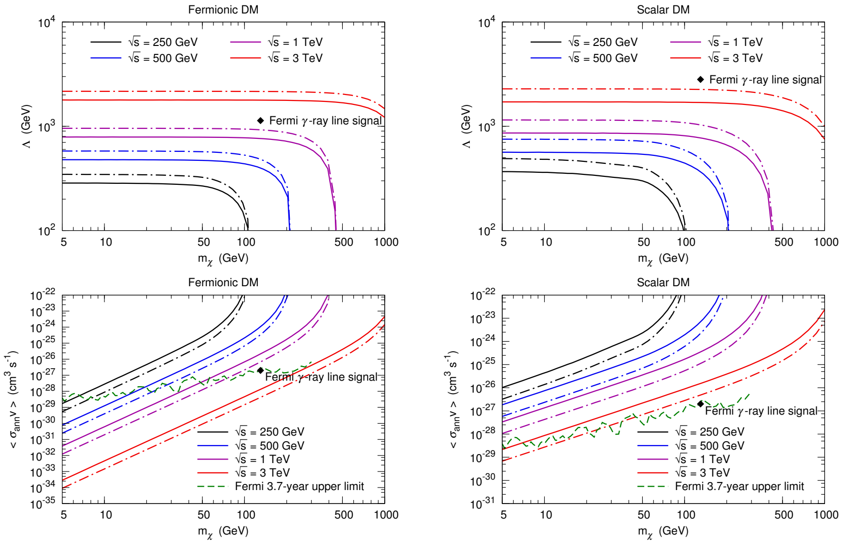

Solid lines: $100\,\mathrm{fb}^{-1}$; dot-dashed lines: $1000\,\mathrm{fb}^{-1}$ $(S/\sqrt{B} = 3)$

ILC luminosity: $240 - 570\,\mathrm{fb}^{-1}/\mathrm{year}$ [ILC TDR, Vol. 1, 1306.6327]

Beam Polarization

For a process at an e^+e^- collider with **polarized beams**,

$$\sigma(P_{e^-}, P_{e^+}) = \frac{1}{4}\Big[(1+P_{e^-})(1+P_{e^+})\sigma_{\rm RR} + (1-P_{e^-})(1-P_{e^+})\sigma_{\rm LL} + (1+P_{e^-})(1-P_{e^+})\sigma_{\rm RL} + (1-P_{e^-})(1+P_{e^+})\sigma_{\rm LR}\Big]$$

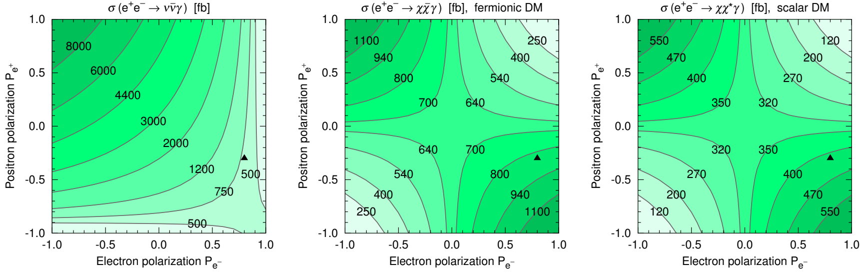

▲ $(P_{e^-}, P_{e^+}) = (0.8, -0.3)$ **can be achieved at the ILC**

[ILC technical design report, Vol. 1, 1306.6327]

Improvement from Beam Polarization

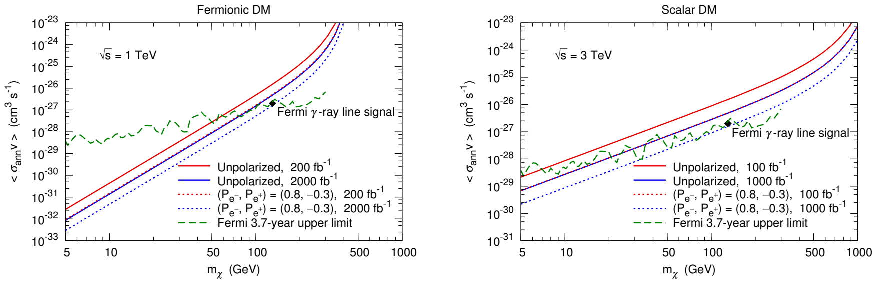

$(S/\sqrt{B} = 3)$

Using the **polarized beams** is roughly equivalent to **increasing** the integrated luminosity by **an order of magnitude**.

For fermionic DM (scalar DM), a data set of $2000\,\mathrm{fb}^{-1}$ $(1000\,\mathrm{fb}^{-1})$ would be just sufficient to test the Fermi γ-ray line signal at an e^+e^- collider with $\sqrt{s} = 1\,\mathrm{TeV}$ $(3\,\mathrm{TeV})$.

Mono-Z Searches at e^+e^- Colliders

PHYSICAL REVIEW D **90,** 055010 (2014)

Dark matter searches in the mono-Z channel at high energy e^+e^- colliders

Zhao-Huan Yu,[1] Xiao-Jun Bi,[1] Qi-Shu Yan,[2,3] and Peng-Fei Yin[1]

[1] *Key Laboratory of Particle Astrophysics, Institute of High Energy Physics, Chinese Academy of Sciences, Beijing 100049, China*

[2] *School of Physics, University of Chinese Academy of Sciences, Beijing 100049, China*

[3] *Center for High Energy Physics, Peking University, Beijing 100871, China*

(Received 14 May 2014; published 10 September 2014)

We explore the mono-Z signature for dark matter searches at future high energy e^+e^- colliders. In the context of effective field theory, we consider two kinds of contact operators describing dark matter interactions with electroweak gauge bosons and with electron/positron, respectively. For five benchmark models, we propose kinematic cuts to distinguish signals from backgrounds for both charged leptonic and hadronic decay modes of the Z boson. We also present the experimental sensitivity to cutoff scales of effective operators and compare it with that of the Fermi-LAT indirect search and demonstrate the gains in significance for the several configurations of polarized beams.

DOI: 10.1103/PhysRevD.90.055010 PACS numbers: 95.35.+d, 12.60.-i, 13.66.Hk

[arXiv:1404.6990, PRD]

Mono-Z Signature: DM Couplings to $ZZ/Z\gamma$

The mono-Z channel at high energy e^+e^- collider can be sensitive to **the DM coupling to $ZZ/Z\gamma$.**

Assuming the DM particle χ is a Dirac fermion, we consider the following effective operators:

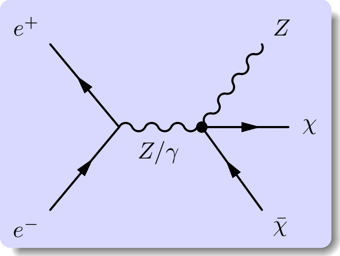

$$\mathcal{O}_{\mathrm{F1}} = \frac{1}{\Lambda_1^3}\bar{\chi}\chi B_{\mu\nu}B^{\mu\nu} + \frac{1}{\Lambda_2^3}\bar{\chi}\chi W^a_{\mu\nu}W^{a\mu\nu}$$
$$\supset \bar{\chi}\chi(G_{\mathrm{ZZ}}Z_{\mu\nu}Z^{\mu\nu} + G_{\mathrm{AZ}}A_{\mu\nu}Z^{\mu\nu})$$

$$\mathcal{O}_{\mathrm{F2}} = \frac{1}{\Lambda_1^3}\bar{\chi}i\gamma_5\chi B_{\mu\nu}\tilde{B}^{\mu\nu} + \frac{1}{\Lambda_2^3}\bar{\chi}i\gamma_5\chi W^a_{\mu\nu}\tilde{W}^{a\mu\nu}$$
$$\supset \bar{\chi}i\gamma_5\chi(G_{\mathrm{ZZ}}Z_{\mu\nu}\tilde{Z}^{\mu\nu} + G_{\mathrm{AZ}}A_{\mu\nu}\tilde{Z}^{\mu\nu})$$

$$G_{\mathrm{ZZ}} \equiv \frac{\sin^2\theta_W}{\Lambda_1^3} + \frac{\cos^2\theta_W}{\Lambda_2^3}$$

$$\mathcal{O}_{\mathrm{FH}} = \frac{1}{\Lambda^3}\bar{\chi}\chi(D_\mu H)^\dagger D_\mu H \to \frac{m_Z^2}{2\Lambda^3}\bar{\chi}\chi Z_\mu Z^\mu$$

$$G_{\mathrm{AZ}} \equiv 2\sin\theta_W\cos\theta_W\left(\frac{1}{\Lambda_2^3} - \frac{1}{\Lambda_1^3}\right)$$

Mono-Z Signature: DM Couplings to e^+e^-

This channel can also be sensitive to **the DM coupling to e^+e^-.**

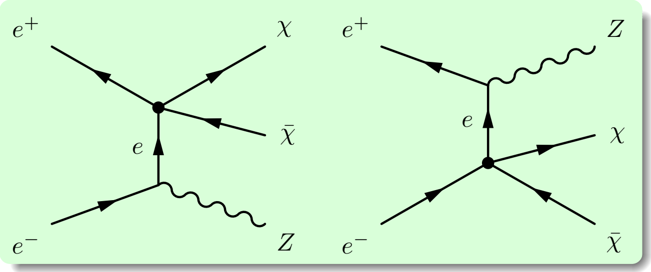

We consider the following effective operators:

$$\mathcal{O}_{\rm FP} = \frac{1}{\Lambda^2}\bar{\chi}\gamma_5\chi\bar{e}\gamma_5 e, \qquad \mathcal{O}_{\rm FA} = \frac{1}{\Lambda^2}\bar{\chi}\gamma^\mu\gamma_5\chi\bar{e}\gamma_\mu\gamma_5 e$$

MC Simulation

Simulation tools: FeynRules → MadGraph → PYTHIA → PGS

SiD/ILD-like detector:

ECAL energy resolution $\dfrac{\Delta E}{E} = \dfrac{17\%}{\sqrt{E/\text{GeV}}} \oplus 1\%$

HCAL energy resolution $\dfrac{\Delta E}{E} = \dfrac{30\%}{\sqrt{E/\text{GeV}}}$

Collision energies of future e^+e^- colliders:

$\sqrt{s} = 250\,\text{GeV}$: "Higgs factory" (CEPC/TLEP, ILC)

$\sqrt{s} = 500\,\text{GeV}$: typical ILC

$\sqrt{s} = 1\,\text{TeV}$: upgraded ILC

Lepton Channel: $Z \to \ell^+\ell^-$ ($\ell = e, \mu$)

SM backgrounds: $e^+e^- \to \ell^+\ell^-\bar{\nu}\nu$, $e^+e^- \to \tau^+\tau^-$, $e^+e^- \to \tau^+\tau^-\bar{\nu}\nu$

Lepton Channel: $Z \to \ell^+\ell^-$ ($\ell = e, \mu$)

SM backgrounds: $e^+e^- \to \ell^+\ell^-\bar{\nu}\nu$, $e^+e^- \to \tau^+\tau^-$, $e^+e^- \to \tau^+\tau^-\bar{\nu}\nu$

Reconstructing the Z boson: require only 2 leptons (e's or μ's) with $p_{\mathrm{T}} > 10$ GeV and $|\eta| < 3$, and they are opposite sign and same flavor;
no any other particle;

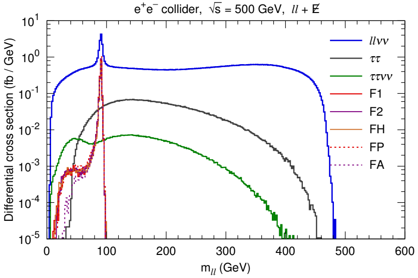

Lepton Channel: $Z \to \ell^+\ell^-$ ($\ell = e, \mu$)

SM backgrounds: $e^+e^- \to \ell^+\ell^-\bar{\nu}\nu$, $e^+e^- \to \tau^+\tau^-$, $e^+e^- \to \tau^+\tau^-\bar{\nu}\nu$

Reconstructing the Z boson: require only 2 leptons (e's or μ's) with $p_T > 10$ GeV and $|\eta| < 3$, and they are opposite sign and same flavor; **no any other particle;** require the invariant mass of the 2 leptons satisfying $|m_{\ell\ell} - m_Z| < 5$ GeV.

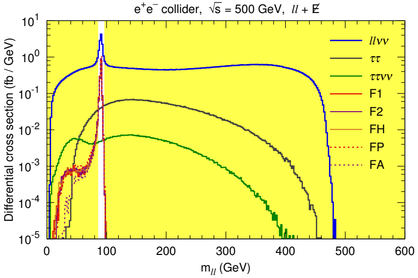

Lepton Channel: $Z \to \ell^+\ell^-$ $(\ell = e, \mu)$

SM backgrounds: $e^+e^- \to \ell^+\ell^-\bar{\nu}\nu$, $e^+e^- \to \tau^+\tau^-$, $e^+e^- \to \tau^+\tau^-\bar{\nu}\nu$

Reconstructing the Z boson: require only 2 leptons (e's or μ's) with $p_\mathrm{T} > 10$ GeV and $|\eta| < 3$, and they are opposite sign and same flavor; **no any other particle;** require the invariant mass of the 2 leptons satisfying $|m_{\ell\ell} - m_Z| < 5$ GeV.

Reconstructing the recoil mass: $m_\mathrm{recoil} = \sqrt{(p_{e^+} + p_{e^-} - p_{\ell_1} - p_{\ell_2})^2}$;

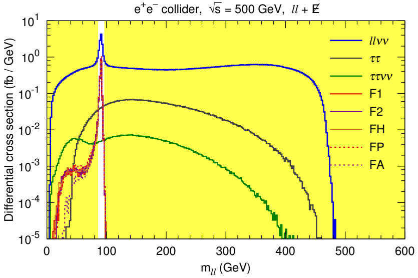

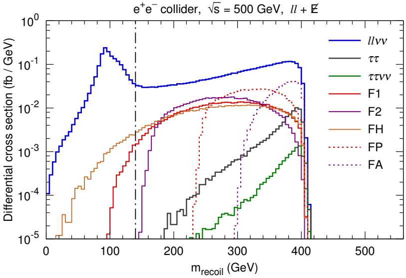

Lepton Channel: $Z \to \ell^+\ell^-$ ($\ell = e, \mu$)

SM backgrounds: $e^+e^- \to \ell^+\ell^-\bar{\nu}\nu$, $e^+e^- \to \tau^+\tau^-$, $e^+e^- \to \tau^+\tau^-\bar{\nu}\nu$

Reconstructing the Z boson: require only 2 leptons (e's or μ's) with $p_{\mathrm{T}} > 10$ GeV and $|\eta| < 3$, and they are opposite sign and same flavor; **no any other particle;** require the invariant mass of the 2 leptons satisfying $|m_{\ell\ell} - m_Z| < 5$ GeV.

Reconstructing the recoil mass: $m_{\mathrm{recoil}} = \sqrt{(p_{e^+} + p_{e^-} - p_{\ell_1} - p_{\ell_2})^2}$; veto events with $m_{\mathrm{recoil}} < 140$ GeV.

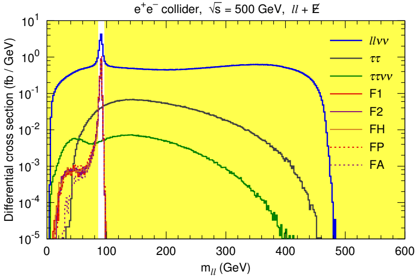

Lepton Channel: $Z \to \ell^+\ell^-$ ($\ell = e, \mu$)

Cross sections σ and signal significances $\mathcal{S}$ after each cut

($\sqrt{s} = 500$ GeV, with an integrated luminosity of 100 fb^{-1})

	$\ell^+\ell^-\bar{\nu}\nu$	$\tau^+\tau^-$	$\tau^+\tau^-\bar{\nu}\nu$	$\mathcal{O}_{\rm F1}$		$\mathcal{O}_{\rm F2}$		$\mathcal{O}_{\rm FH}$		$\mathcal{O}_{\rm FP}$		$\mathcal{O}_{\rm FA}$	
	σ	σ	σ	σ	$\mathcal{S}$	σ	$\mathcal{S}$	σ	$\mathcal{S}$	σ	$\mathcal{S}$	σ	$\mathcal{S}$
Cut 1	**306**	**20.4**	**2.85**	2.65	1.46	2.94	1.61	2.47	1.36	3.24	1.78	2.86	1.57
Cut 2	235	11.8	1.29	2.52	1.60	2.82	1.78	2.39	1.51	3.19	2.01	2.19	1.38
Cut 3	23.9	0.410	0.0495	2.41	4.67	2.70	5.18	2.29	4.44	3.06	5.84	2.09	4.07
Cut 4	16.0	0.410	0.0495	2.39	5.51	2.70	6.16	2.19	5.08	3.06	6.92	2.09	4.86
Cut 5	**12.1**	**0.410**	**0.0471**	2.19	5.69	2.42	6.24	2.11	5.50	2.95	7.47	2.01	5.25

(σ in fb, $\mathcal{S} = S/\sqrt{S+B}$)

Hadron Channel: $Z \to jj$

SM backgrounds: $e^+e^- \to jj\bar{\nu}\nu$, $e^+e^- \to jj\ell\nu$, $e^+e^- \to t\bar{t}$

Hadron Channel: $Z \to jj$

SM backgrounds: $e^+e^- \to jj\bar{\nu}\nu$, $e^+e^- \to jj\ell\nu$, $e^+e^- \to t\bar{t}$

Reconstructing the Z boson: require only 2 jets with $p_T > 10$ GeV and $|\eta| < 3$; **no any other particle;**

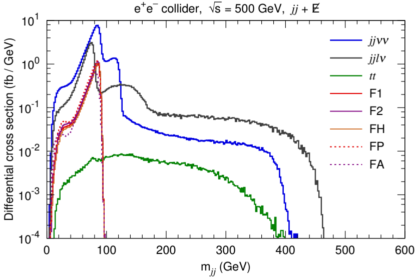

Hadron Channel: $Z \to jj$

SM backgrounds: $e^+e^- \to jj\bar{\nu}\nu$, $e^+e^- \to jj\ell\nu$, $e^+e^- \to t\bar{t}$

Reconstructing the Z boson: require only 2 jets with $p_T > 10$ GeV and $|\eta| < 3$; **no any other particle;** require the invariant mass of the 2 jets satisfying 40 GeV $< m_{jj} <$ 95 GeV.

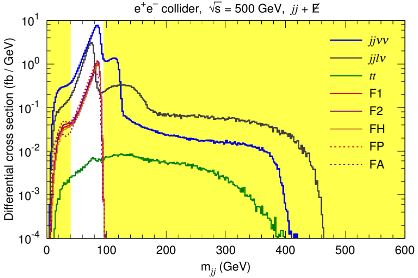

Hadron Channel: $Z \to jj$

SM backgrounds: $e^+e^- \to jj\bar{\nu}\nu$, $e^+e^- \to jj\ell\nu$, $e^+e^- \to t\bar{t}$

Reconstructing the Z boson: require only 2 jets with $p_{\mathrm{T}} > 10$ GeV and $|\eta| < 3$; **no any other particle;** require the invariant mass of the 2 jets satisfying 40 GeV $< m_{jj} <$ 95 GeV.

Reconstructing the recoil mass: $m_{\mathrm{recoil}} = \sqrt{(p_{e^+} + p_{e^-} - p_{j_1} - p_{j_2})^2}$;

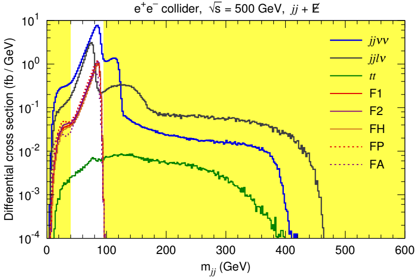

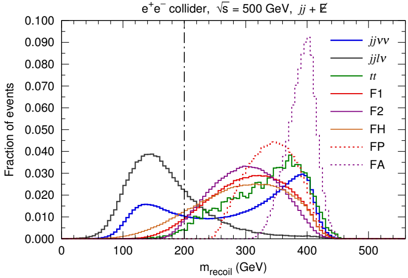

Hadron Channel: $Z \to jj$

SM backgrounds: $e^+e^- \to jj\bar{\nu}\nu$, $e^+e^- \to jj\ell\nu$, $e^+e^- \to t\bar{t}$

Reconstructing the Z boson: require only 2 jets with $p_{\mathrm{T}} > 10$ GeV and $|\eta| < 3$; **no any other particle;** require the invariant mass of the 2 jets satisfying 40 GeV $< m_{jj} <$ 95 GeV.

Reconstructing the recoil mass: $m_{\mathrm{recoil}} = \sqrt{(p_{e^+} + p_{e^-} - p_{j_1} - p_{j_2})^2}$; veto events with $m_{\mathrm{recoil}} <$ 200 GeV.

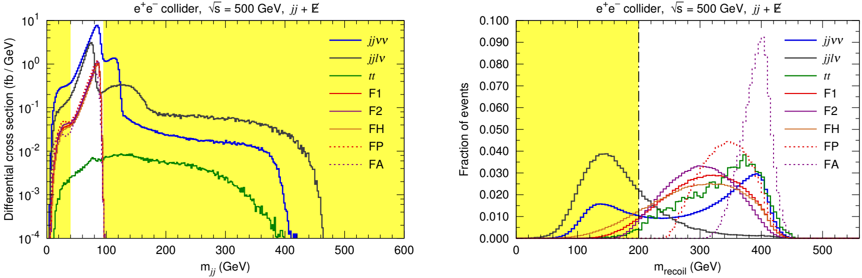

Hadron Channel: $Z \to jj$

Cross sections σ and signal significances $\mathcal{S}$ after each cut

($\sqrt{s} = 500$ GeV, with an integrated luminosity of 100 fb^{-1})

	$jj\nu\bar{\nu}$	$jj\ell\nu$	$t\bar{t}$	$\mathcal{O}_{\rm F1}$		$\mathcal{O}_{\rm F2}$		$\mathcal{O}_{\rm FH}$		$\mathcal{O}_{\rm FP}$		$\mathcal{O}_{\rm FA}$	
	σ	σ	σ	σ	$\mathcal{S}$	σ	$\mathcal{S}$	σ	$\mathcal{S}$	σ	$\mathcal{S}$	σ	$\mathcal{S}$
Cut 1	**245**	**131**	**1.74**	18.9	9.47	20.9	10.4	17.8	8.94	22.1	11.1	18.4	9.24
Cut 2	207	93.2	1.56	18.0	10.0	20.0	11.2	17.2	9.64	21.8	12.1	13.9	7.84
Cut 3	160	56.6	0.270	17.2	11.2	19.2	12.5	16.6	10.8	20.7	13.5	13.3	8.76
Cut 4	115	14.9	0.264	16.3	13.4	18.7	15.3	14.6	12.1	20.7	16.9	13.3	11.1
Cut 5	**92.6**	**2.91**	**0.253**	15.1	14.3	17.1	16.1	14.1	13.5	20.1	18.7	12.9	12.3

(σ in fb, $\mathcal{S} = S/\sqrt{S+B}$)

3σ Sensitivity: DM Couplings to $ZZ/Z\gamma$

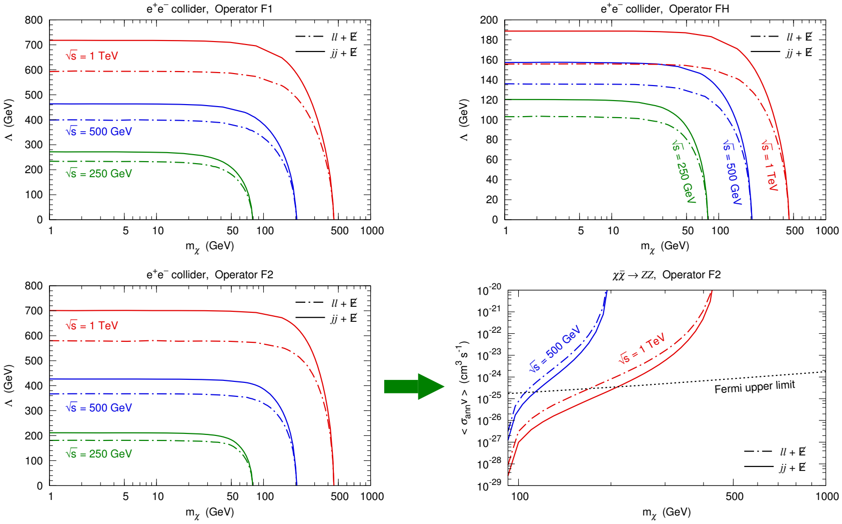

(with an integrated luminosity of 1000 fb^{-1}, assuming $\Lambda = \Lambda_1 = \Lambda_2$ for $\mathcal{O}_{\mathrm{F1}}$ and $\mathcal{O}_{\mathrm{F2}}$)

3σ Sensitivity Affected by the Λ_1-Λ_2 Relation

$\chi\chi ZZ$ coupling:

$$G_{ZZ} = \frac{\sin^2\theta_W}{\Lambda_1^3} + \frac{\cos^2\theta_W}{\Lambda_2^3}$$

$\chi\chi\gamma Z$ coupling:

$$G_{AZ} = 2\sin\theta_W\cos\theta_W\left(\frac{1}{\Lambda_2^3} - \frac{1}{\Lambda_1^3}\right)$$

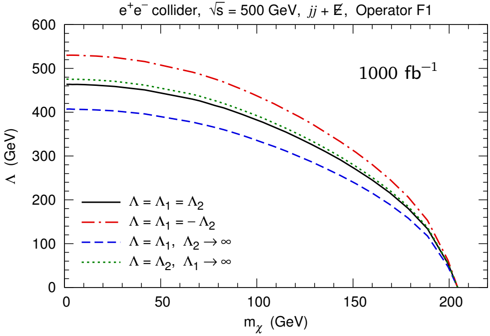

$\Lambda = \Lambda_1 = \Lambda_2$: only the $\chi\chi ZZ$ coupling contributes.

$\Lambda = \Lambda_1 = -\Lambda_2$: the $\chi\chi\gamma Z$ coupling is dominant.

$\Lambda = \Lambda_1,\ \Lambda_2 \to \infty$: the $\chi\chi\gamma Z$ coupling is dominant.

$\Lambda = \Lambda_2,\ \Lambda_1 \to \infty$: the $\chi\chi ZZ$ and the $\chi\chi\gamma Z$ couplings are comparable.

3σ Sensitivity: DM Couplings to e^+e^-

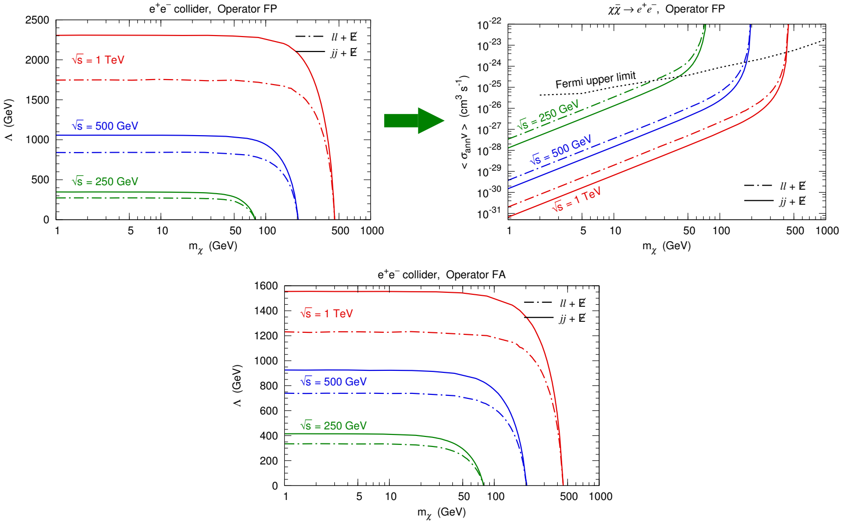

(with an integrated luminosity of 1000 fb^{-1}; Fermi upper limits come from arXiv:1310.0828)

Cross Sections with Polarized Beams

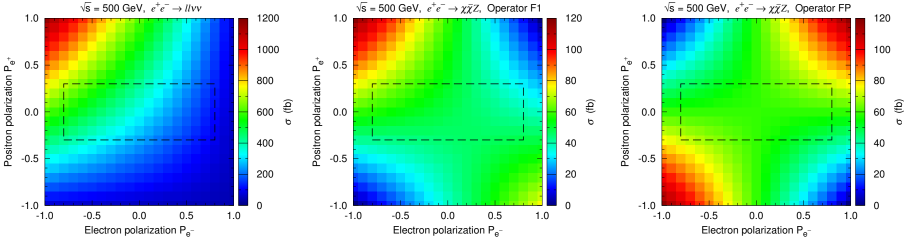

($\ell\ell\bar{\nu}\nu$, $jj\bar{\nu}\nu$, $jj\ell\nu$ are similar) ($\mathcal{O}_{\mathrm{F1}}$, $\mathcal{O}_{\mathrm{F2}}$, $\mathcal{O}_{\mathrm{FH}}$, $\mathcal{O}_{\mathrm{FA}}$ are similar) ($\mathcal{O}_{\mathrm{FP}}$)

- $W^\pm$ only couples to left-handed e^- (right-handed e^+).
- $e^\pm$ couples to Z^0 via $\dfrac{g_2}{2\cos\theta_W}(g_L\bar{e}_L\gamma^\mu e_L + g_R\bar{e}_R\gamma^\mu e_R)Z_\mu$.

  $g_L = -1 + 2\sin^2\theta_W \simeq -0.56$, $g_R = 2\sin^2\theta_W \simeq 0.44$, $g_L^2/g_R^2 \simeq 1.56$.

  The left-handed e^- (right-handed e^+) coupling to Z^0 is stronger.

Cross Sections with Polarized Beams

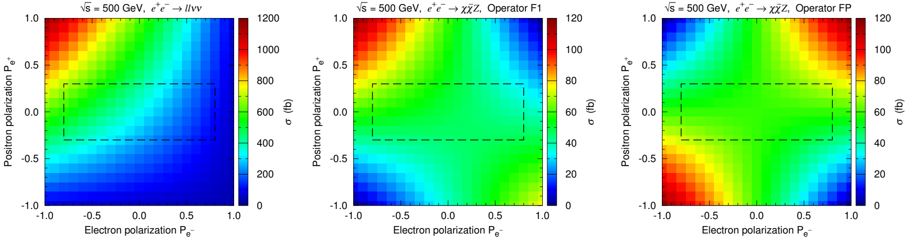

($\ell\ell\bar{\nu}\nu$, $jj\bar{\nu}\nu$, $jj\ell\nu$ are similar) ($\mathcal{O}_{\mathrm{F1}}$, $\mathcal{O}_{\mathrm{F2}}$, $\mathcal{O}_{\mathrm{FH}}$, $\mathcal{O}_{\mathrm{FA}}$ are similar) ($\mathcal{O}_{\mathrm{FP}}$)

The dashed box indicates the polarization ranges achievable at the ILC:

$$-0.8 \le P_{e^-} \le +0.8, \quad -0.3 \le P_{e^+} \le +0.3.$$

In order to obtain the maximal signal significance,

Cross Sections with Polarized Beams

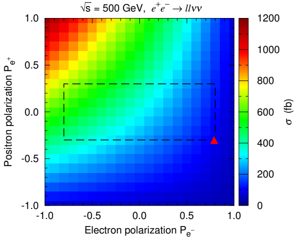

($\ell\ell\bar{\nu}\nu$, $jj\bar{\nu}\nu$, $jj\ell\nu$ are similar)

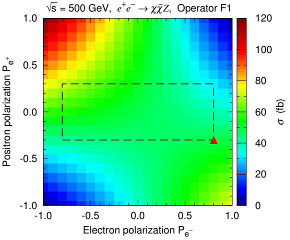

($\mathcal{O}_{\rm F1}$, $\mathcal{O}_{\rm F2}$, $\mathcal{O}_{\rm FH}$, $\mathcal{O}_{\rm FA}$ are similar)

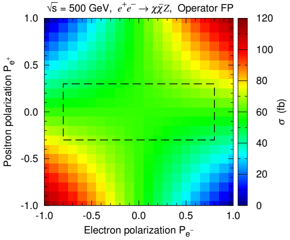

($\mathcal{O}_{\rm FP}$)

The dashed box indicates the polarization ranges achievable at the ILC:

$$-0.8 \le P_{e^-} \le +0.8, \quad -0.3 \le P_{e^+} \le +0.3.$$

In order to obtain the maximal signal significance,

▲ $(P_{e^-}, P_{e^+}) = (+0.8, -0.3)$ is optimal for $\mathcal{O}_{\rm F1}$, $\mathcal{O}_{\rm F2}$, $\mathcal{O}_{\rm FH}$, $\mathcal{O}_{\rm FA}$;

Cross Sections with Polarized Beams

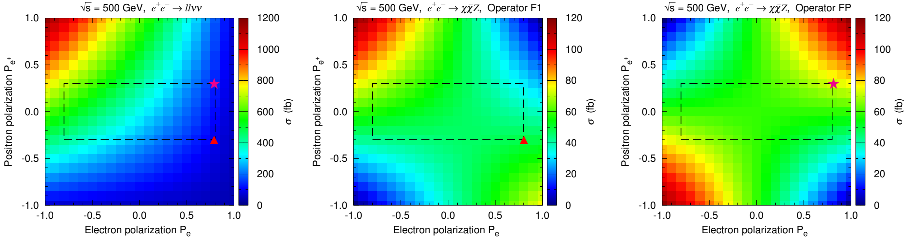

($\ell\ell\bar{\nu}\nu$, $jj\bar{\nu}\nu$, $jj\ell\nu$ are similar) ($\mathcal{O}_{\mathrm{F1}}$, $\mathcal{O}_{\mathrm{F2}}$, $\mathcal{O}_{\mathrm{FH}}$, $\mathcal{O}_{\mathrm{FA}}$ are similar) ($\mathcal{O}_{\mathrm{FP}}$)

The dashed box indicates the polarization ranges achievable at the ILC:

$$-0.8 \le P_{e^-} \le +0.8, \quad -0.3 \le P_{e^+} \le +0.3.$$

In order to obtain the maximal signal significance,

▲ $(P_{e^-}, P_{e^+}) = (+0.8, -0.3)$ is optimal for $\mathcal{O}_{\mathrm{F1}}$, $\mathcal{O}_{\mathrm{F2}}$, $\mathcal{O}_{\mathrm{FH}}$, $\mathcal{O}_{\mathrm{FA}}$;

★ $(P_{e^-}, P_{e^+}) = (+0.8, +0.3)$ is optimal for $\mathcal{O}_{\mathrm{FP}}$.

Sensitivity Improvement

Signal significances without and **with** polarized beams for the benchmark points at $\sqrt{s} = 500$ GeV ($100\ \text{fb}^{-1}$):

Lepton channel $\ell^+\ell^- + \not{E}$

	$\mathcal{S}_{\text{unpol}}$	$\mathcal{S}_{\text{pol}}$	$\mathcal{S}_{\text{pol}}/\mathcal{S}_{\text{unpol}}$
$\mathcal{O}_{\text{F1}}$	5.69	10.1	**1.78**
$\mathcal{O}_{\text{F2}}$	6.24	10.9	**1.75**
$\mathcal{O}_{\text{FH}}$	5.50	9.70	**1.76**
$\mathcal{O}_{\text{FP}}$	7.47	13.4	**1.79**
$\mathcal{O}_{\text{FA}}$	5.25	9.29	**1.77**

Hadron channel $jj + \not{E}$

	$\mathcal{S}_{\text{unpol}}$	$\mathcal{S}_{\text{pol}}$	$\mathcal{S}_{\text{pol}}/\mathcal{S}_{\text{unpol}}$
$\mathcal{O}_{\text{F1}}$	14.3	26.0	**1.82**
$\mathcal{O}_{\text{F2}}$	16.1	28.6	**1.78**
$\mathcal{O}_{\text{FH}}$	13.5	24.8	**1.84**
$\mathcal{O}_{\text{FP}}$	18.7	34.4	**1.84**
$\mathcal{O}_{\text{FA}}$	12.3	23.0	**1.87**

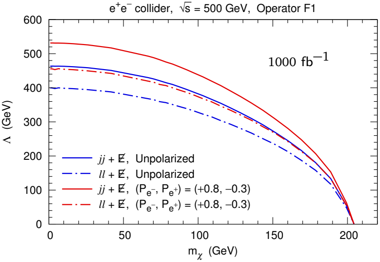

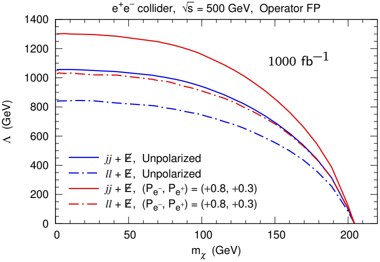

Indirectly Probing Dark Matter via EW Oblique Parameters

ELSEVIER
Nuclear Physics B 921 (2017) 181–210
www.elsevier.com/locate/nuclphysb

CEPC precision of electroweak oblique parameters and weakly interacting dark matter: The fermionic case

Chengfeng Cai [a,1], Zhao-Huan Yu [b,1], Hong-Hao Zhang [a,*]

[a] School of Physics, Sun Yat-Sen University, Guangzhou 510275, China
[b] ARC Centre of Excellence for Particle Physics at the Terascale, School of Physics, The University of Melbourne, Victoria 3010, Australia

[arXiv:1611.02186, NPB]

CEPC Precision of Electroweak Oblique Parameters and Weakly Interacting Dark Matter: the Scalar Case

Chengfeng Cai,[a] **Zhao-Huan Yu,**[b] **and Hong-Hao Zhang**[1a]

[a] *School of Physics, Sun Yat-Sen University, Guangzhou 510275, China*
[b] *ARC Centre of Excellence for Particle Physics at the Terascale, School of Physics, The University of Melbourne, Victoria 3010, Australia*

[arXiv:1705.07921]

CEPC Project

The **Circular Electron Positron Collider (CEPC)**, proposed by the Chinese HEP community, will mainly serve as a Higgs factory at $\sqrt{s} \sim 240$ GeV

The **preliminary conceptual design report** was released in May 2015:
`http://cepc.ihep.ac.cn/preCDR/volume.html`

Its low-energy plans will operate at the Z pole ($\sqrt{s} \sim 91$ GeV, 10^{10} Z bosons) and near the WW threshold ($\sqrt{s} \sim 160$ GeV), leading to great improvements for **electroweak (EW) precision measurements**

WIMP models typically contain colorless **EW multiplets** whose electrically neutral components serve as DM candidates; such multiplets will affect EW precision observables (or **oblique parameters**) via **loop corrections**

$\Downarrow$

CEPC provides an excellent opportunity to indirectly probe WIMP DM models

Electroweak Radiative Corrections

Two classes of EW radiative corrections

- **Direct Corrections:** vertex, box, and bremsstrahlung corrections

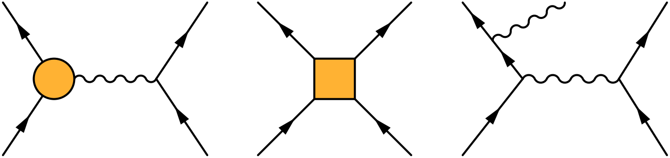

- **Oblique Corrections:** gauge boson propagator corrections

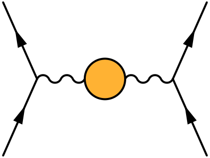

Oblique corrections can be treated in a self-consistent and model-independent way through an effective lagrangian to incorporate a large class of Feynman diagrams into a few **running couplings** [Kennedy & Lynn, NPB 322, 1 (1989)]

Electroweak Oblique Parameters

EW oblique parameters S, T, and U are further introduced to describe **new physics contributions** through oblique corrections [Peskin & Takeuchi, '90, '92]

$$S = 16\pi[\Pi'_{33}(0) - \Pi'_{3Q}(0)]$$

$$T = \frac{4\pi}{s_W^2 c_W^2 m_Z^2}[\Pi_{11}(0) - \Pi_{33}(0)], \quad U = 16\pi[\Pi'_{11}(0) - \Pi'_{33}(0)]$$

Here $\Pi'_{IJ}(0) \equiv \partial \Pi_{IJ}(p^2)/\partial p^2|_{p^2=0}$, $s_W \equiv \sin\theta_W$, $c_W \equiv \cos\theta_W$

γ  γ

$$= ie^2 \Pi_{QQ}(p^2) g^{\mu\nu} + (p^\mu p^\nu \text{ terms})$$

Z  γ

$$= \frac{ie^2}{s_W c_W}[\Pi_{3Q}(p^2) - s_W^2 \Pi_{QQ}(p^2)] g^{\mu\nu} + (p^\mu p^\nu \text{ terms})$$

Z  Z

$$= \frac{ie^2}{s_W^2 c_W^2}[\Pi_{33}(p^2) - 2 s_W^2 \Pi_{3Q}(p^2) + s_W^4 \Pi_{QQ}(p^2)] g^{\mu\nu} + (p^\mu p^\nu \text{ terms})$$

W  W

$$= \frac{ie^2}{s_W^2} \Pi_{11}(p^2) g^{\mu\nu} + (p^\mu p^\nu \text{ terms})$$

Custodial Symmetry

Standard model (SM) scalar potential $V = -\mu^2 H^\dagger H + \lambda(H^\dagger H)^2$ is a function of $H^\dagger H$, which respects an $\mathrm{SU}(2)_\mathrm{L} \times \mathrm{SU}(2)_\mathrm{R}$ **global symmetry**:

$$H^\dagger H = -\frac{1}{2}\epsilon_{AB}\epsilon^{ij}(\mathcal{H}^A)_i(\mathcal{H}^B)_j, \quad (\mathcal{H}^A)_i \equiv \begin{pmatrix} H_i^\dagger \\ H_i \end{pmatrix} \text{ is an } \mathrm{SU}(2)_\mathrm{R} \text{ doublet}$$

$$H \to \frac{1}{\sqrt{2}}\begin{pmatrix} 0 \\ v \end{pmatrix} \quad \Rightarrow \quad \mathrm{SU}(2)_\mathrm{L} \times \mathrm{SU}(2)_\mathrm{R} \to \mathrm{SU}(2)_{\mathrm{L+R}} \text{ custodial symmetry}$$

$\Downarrow$

$\mathrm{SU}(2)_\mathrm{L}$ gauge bosons W^a_μ transform as an $\mathrm{SU}(2)_{\mathrm{L+R}}$ triplet and acquire the same mass from EW symmetry breaking

$\Downarrow$

The custodial symmetry protects the tree-level relation $\rho \equiv m_W^2/(m_Z^2 c_\mathrm{W}^2) = 1$ up to EW radiative corrections [Sikivie *et al.*, NPB 173, 189 (1980)], and leads to $T = U = 0$ (note that $\rho - 1 = \alpha T$)

The custodial symmetry is **approximate** in the SM, explicitly broken by the Yukawa couplings of fermions and the $\mathrm{U}(1)_\mathrm{Y}$ gauge interaction

Electroweak Precision Observables

For evaluating CEPC precision of oblique parameters, we use a simplified set of EW precision observables in the **global fit**:

$$\alpha_s(m_Z^2),\ \Delta\alpha_{\text{had}}^{(5)}(m_Z^2),\ m_Z,\ m_t,\ m_h,\ m_W,\ \sin^2\theta_{\text{eff}}^{\ell},\ \Gamma_Z$$

Free parameters: the former 5 observables, S, T, and U

The remaining 3 observables are determined by the free parameters:

$$m_W = m_W^{\text{SM}}\left[1-\frac{\alpha}{4(c_{\text{W}}^2-s_{\text{W}}^2)}(S-1.55T-1.24U)\right]$$

$$\sin^2\theta_{\text{eff}}^{\ell} = (\sin^2\theta_{\text{eff}}^{\ell})^{\text{SM}}+\frac{\alpha}{4(c_{\text{W}}^2-s_{\text{W}}^2)}(S-0.69T)$$

$$\Gamma_Z = \Gamma_Z^{\text{SM}}-\frac{\alpha^2 m_Z}{72 s_{\text{W}}^2 c_{\text{W}}^2(c_{\text{W}}^2-s_{\text{W}}^2)}(12.2S-32.9T)$$

The calculation of **SM predictions** is based on 2-loop radiative corrections

CEPC Precision of Electroweak Observables

	Current data	CEPC-B precision	CEPC-I precision
$\alpha_s(m_Z^2)$	0.1185 ± 0.0006	$\pm 1 \times 10^{-4}$	
$\Delta\alpha_{\text{had}}^{(5)}(m_Z^2)$	0.02765 ± 0.00008	$\pm 4.7 \times 10^{-5}$	
m_Z [GeV]	91.1875 ± 0.0021	$\pm 5 \times 10^{-4}$	$\pm 1 \times 10^{-4}$
m_t [GeV]	$173.34 \pm 0.76_{\text{ex}} \pm 0.5_{\text{th}}$	$\pm 0.2_{\text{ex}} \pm 0.5_{\text{th}}$	$\pm 0.03_{\text{ex}} \pm 0.1_{\text{th}}$
m_h [GeV]	125.09 ± 0.24	$\pm 5.9 \times 10^{-3}$	
m_W [GeV]	$80.385 \pm 0.015_{\text{ex}} \pm 0.004_{\text{th}}$	$(\pm 3_{\text{ex}} \pm 1_{\text{th}}) \times 10^{-3}$	
$\sin^2\theta_{\text{eff}}^{\ell}$	0.23153 ± 0.00016	$(\pm 2.3_{\text{ex}} \pm 1.5_{\text{th}}) \times 10^{-5}$	
Γ_Z [GeV]	2.4952 ± 0.0023	$(\pm 5_{\text{ex}} \pm 0.8_{\text{th}}) \times 10^{-4}$	$(\pm 1_{\text{ex}} \pm 0.8_{\text{th}}) \times 10^{-4}$

For **CEPC baseline (CEPC-B) precisions**, experimental uncertainties will be mostly reduced by CEPC measurements; theoretical uncertainties of m_W, $\sin^2\theta_{\text{eff}}^{\ell}$, and Γ_Z can be reduced by fully calculating 3-loop corrections in the future

CEPC improved (CEPC-I) precisions need

- A high-precision beam energy calibration for improving m_Z and Γ_Z measurements
- A $t\bar{t}$ threshold scan for the m_t measurement at other e^+e^- colliders, like ILC

Global Fit

We use a **modified χ^2 function** [Fan, Reece & Wang, 1411.1054] for the global fit:

$$\sum_i \left(\frac{O_i^{\text{meas}} - O_i^{\text{pred}}}{\sigma_i} \right)^2 + \sum_j \left\{ -2\ln \left[\text{erf}\left(\frac{O_j^{\text{meas}} - O_j^{\text{pred}} + \delta_j}{\sqrt{2}\sigma_j} \right) - \text{erf}\left(\frac{O_j^{\text{meas}} - O_j^{\text{pred}} - \delta_j}{\sqrt{2}\sigma_j} \right) \right] \right\}$$

The **experimental uncertainty** σ_j and the **theoretical uncertainty** δ_j of an observable O_j are treated as **Gaussian** and **flat** errors

	Current	CEPC-B	CEPC-I
σ_S	0.10	0.021	0.011
σ_T	0.12	0.026	0.0071
σ_U	0.094	0.020	0.010
ρ_{ST}	+0.89	+0.90	+0.74
ρ_{SU}	−0.55	−0.68	+0.15
ρ_{TU}	−0.80	−0.84	−0.21

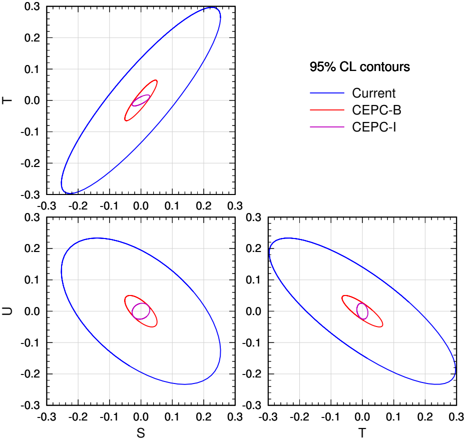

Fit Results for Some Parameters Fixed to 0

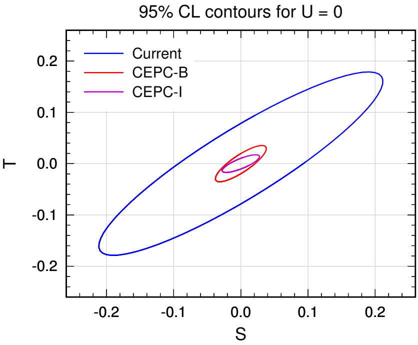

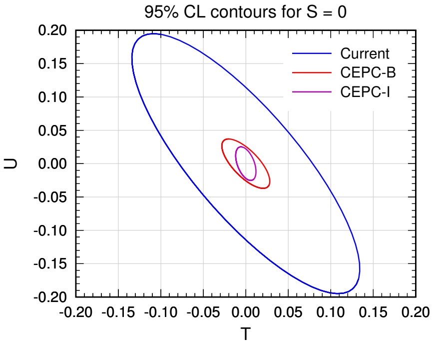

$T = U = 0$ fixed

	Current	CEPC-B	CEPC-I
σ_S	0.037	0.0085	0.0068

$S = U = 0$ fixed

	Current	CEPC-B	CEPC-I
σ_T	0.032	0.0079	0.0042

DM Models with Electroweak Multiplets

We study the CEPC sensitivity to WIMP models with a dark sector consisting of **EW multiplets**. By imposing a Z_2 symmetry, the DM candidate would be the lightest mass eigenstate of the neutral components.

1. EW oblique parameters S, T, and U respond to **EW symmetry breaking**
   - **Mass splittings** among the multiplet components induced by the nonzero Higgs VEV would break the EW symmetry

     $\Rightarrow$ **Nonzero oblique parameters**
   - If the Higgs VEV just gives a **common mass shift** to every components in a multiplet, the effect can be absorbed into the gauge-invariant mass term

     $\Rightarrow$ No EW symmetry breaking effect manifests

     $\Rightarrow$ **Vanishing S, T, and U**
2. S relates to the $\mathrm{U}(1)_\mathrm{Y}$ gauge field

   $\Rightarrow$ A multiplet with **zero hypercharge cannot contribute to S**
3. Multiplet couplings to the Higgs respect a **custodial symmetry**

   $\Rightarrow$ **Vanishing T and U**

Fermionic and Scalar Multiplets

In other to have nonzero contributions to EW oblique parameters, **dark sector multiplets should couple to the SM Higgs doublet**

1. **Fermionic multiplets**
   - **1 vector-like fermionic $\mathrm{SU}(2)_\mathrm{L}$ multiplet:** the Z_2 symmetry for stabilizing DM forbids the multiplet coupling to the Higgs $\quad \Rightarrow \quad S = T = U = 0$
   - **2 types of vector-like $\mathrm{SU}(2)_\mathrm{L}$ multiplets whose dimensions differ by one:** Yukawa couplings split the components $\quad \Rightarrow \quad$ Nonzero oblique parameters
2. **Scalar multiplets**
   - **1 real scalar multiplet Φ:** the quartic coupling $\lambda' \Phi^\dagger \Phi H^\dagger H$ can only induce a common mass shift $\quad \Rightarrow \quad S = T = U = 0$
   - **1 complex scalar multiplet Φ:** the quartic coupling $\lambda'' \Phi^\dagger \tau^a \Phi H^\dagger \sigma^a H$ can induce mass splittings $\quad \Rightarrow \quad$ Nonzero oblique parameters
   - **≥ 2 scalar multiplets:** various trilinear and quartic couplings could break the mass degeneracy $\quad \Rightarrow \quad$ Nonzero oblique parameters

Direct Detection

For a **Majorana DM candidate** χ, the couplings to the Higgs and Z bosons

$$\mathcal{L} \supset \frac{1}{2} g_{h\chi\chi} h \bar{\chi}\chi + \frac{1}{2} g_{Z\chi\chi} Z_\mu \bar{\chi}\gamma^\mu\gamma_5\chi$$

would induce **spin-independent (SI)** and **spin-dependent (SD)** DM-nucleus scatterings.

For scalar multiplets, interactions with the Higgs doublet could split the real and imaginary parts of neutral components, leading to a **CP-even or CP-odd real scalar DM candidate**. Its coupling to the Higgs boson would induce **SI scatterings**.

Most stringent constraints from current direct detection experiments:

- **SI:** PandaX-II [1607.07400], LUX [1608.07648]
- **SD:** PICO (proton) [1503.00008, 1510.07754], LUX (neutron) [1602.03489]

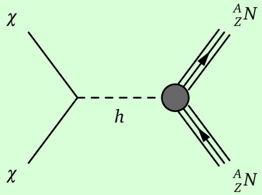

SI for both fermionic and scalar χ

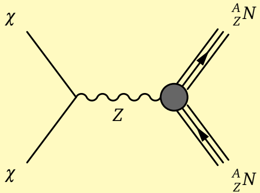

SD for Majorana χ
SI for complex scalar χ

Fermionic Models

Introduce 3 Weyl spinors in the dark sector of each model

1. **Singlet-Doublet Fermionic Dark Matter (SDFDM):**

$$S \in (\mathbf{1}, 0), \quad D_1 = \begin{pmatrix} D_1^0 \\ D_1^- \end{pmatrix} \in (\mathbf{2}, -1/2), \quad D_2 = \begin{pmatrix} D_2^+ \\ D_2^0 \end{pmatrix} \in (\mathbf{2}, +1/2)$$

$$\mathcal{L} \supset -\frac{1}{2} m_S SS - m_D \epsilon_{ij} D_1^i D_2^j + y_1 H_i S D_1^i - y_2 H_i^\dagger S D_2^i + \text{h.c.}$$

2. **Doublet-Triplet Fermionic Dark Matter (DTFDM):**

$$D_1 = \begin{pmatrix} D_1^0 \\ D_1^- \end{pmatrix} \in (\mathbf{2}, -1/2), \quad D_2 = \begin{pmatrix} D_2^+ \\ D_2^0 \end{pmatrix} \in (\mathbf{2}, +1/2), \quad T = \begin{pmatrix} T^+ \\ T^0 \\ T^- \end{pmatrix} \in (\mathbf{3}, 0)$$

$$\mathcal{L} \supset m_D \epsilon_{ij} D_1^i D_2^j - \frac{1}{2} m_T T^a T^a + y_1 H_i T^a (\sigma^a)^i_j D_1^j - y_2 H_i^\dagger T^a (\sigma^a)^i_j D_2^j + \text{h.c.}$$

3. **Triplet-Quadruplet Fermionic Dark Matter (TQFDM):**

$$T = \begin{pmatrix} T^+ \\ T^0 \\ T^- \end{pmatrix} \in (\mathbf{3}, 0), \quad Q_1 = \begin{pmatrix} Q_1^+ \\ Q_1^0 \\ Q_1^- \\ Q_1^{--} \end{pmatrix} \in (\mathbf{4}, -1/2), \quad Q_2 = \begin{pmatrix} Q_2^{++} \\ Q_2^+ \\ Q_2^0 \\ Q_2^- \end{pmatrix} \in (\mathbf{4}, +1/2)$$

$$\mathcal{L} \supset -\frac{1}{2} m_T TT - m_Q Q_1 Q_2 + y_1 \epsilon_{jl} (Q_1)_i^{jk} T_k^i H^l - y_2 (Q_2)_i^{jk} T_k^i H_j^\dagger + \text{h.c.}$$

DTFDM: Detail

Introduce left-handed Weyl fermions in the dark sector:

$$D_1 = \begin{pmatrix} D_1^0 \\ D_1^- \end{pmatrix} \in (\mathbf{2}, -1/2), \quad D_2 = \begin{pmatrix} D_2^+ \\ D_2^0 \end{pmatrix} \in (\mathbf{2}, +1/2), \quad T = \begin{pmatrix} T^+ \\ T^0 \\ T^- \end{pmatrix} \in (\mathbf{3}, 0)$$

$$\mathcal{L}_\mathrm{D} = iD_1^\dagger \bar{\sigma}^\mu D_\mu D_1 + iD_2^\dagger \bar{\sigma}^\mu D_\mu D_2 + (m_D \epsilon_{ij} D_1^i D_2^j + \mathrm{h.c.})$$

$$\mathcal{L}_\mathrm{T} = iT^\dagger \bar{\sigma}^\mu D_\mu T - \frac{1}{2}(m_T T^a T^a + \mathrm{h.c.})$$

Yukawa couplings: $\mathcal{L}_\mathrm{HDT} = y_1 H_i T^a (\sigma^a)^i_j D_1^j - y_2 H_i^\dagger T^a (\sigma^a)^i_j D_2^j + \mathrm{h.c.}$

Custodial symmetry limit $y = y_1 = y_2$ $\Rightarrow$ $\mathrm{SU}(2)_\mathrm{L} \times \mathrm{SU}(2)_\mathrm{R}$ invariant form:

$$\mathcal{L}_\mathrm{D} + \mathcal{L}_\mathrm{HDT} = i\mathcal{D}_A^\dagger \bar{\sigma}^\mu D_\mu \mathcal{D}^A + \frac{1}{2}[m_D \epsilon_{AB} \epsilon_{ij} (\mathcal{D}^A)^i (\mathcal{D}^B)^j + \mathrm{h.c.}] + [y \epsilon_{AB} (\mathcal{H}^A)_i T^a (\sigma^a)^i_j (\mathcal{D}^B)^j + \mathrm{h.c.}]$$

$\mathrm{SU}(2)_\mathrm{R}$ doublets: $(\mathcal{D}^A)^i = \begin{pmatrix} D_1^i \\ D_2^i \end{pmatrix}$, $(\mathcal{H}^A)_i = \begin{pmatrix} H_i^\dagger \\ H_i \end{pmatrix}$

DTFDM: State Mixing

The dark sector involves 3 Majorana fermions and 2 singly charged fermions

$$\mathcal{L}_{\text{mass}} = -\frac{1}{2}(T^0 \quad D_1^0 \quad D_2^0)\mathcal{M}_{\text{N}}\begin{pmatrix} T^0 \\ D_1^0 \\ D_2^0 \end{pmatrix} - (T^- \quad D_1^-)\mathcal{M}_{\text{C}}\begin{pmatrix} T^+ \\ D_2^+ \end{pmatrix} + \text{h.c.}$$

$$= -\frac{1}{2}\sum_{i=1}^{3} m_{\chi_i^0}\chi_i^0\chi_i^0 - \sum_{i=1}^{2} m_{\chi_i^\pm}\chi_i^-\chi_i^+ + \text{h.c.}$$

$$\mathcal{M}_{\text{N}} = \begin{pmatrix} m_T & \frac{1}{\sqrt{2}}y_1 v & -\frac{1}{\sqrt{2}}y_2 v \\ \frac{1}{\sqrt{2}}y_1 v & 0 & m_D \\ -\frac{1}{\sqrt{2}}y_2 v & m_D & 0 \end{pmatrix}, \quad \mathcal{M}_{\text{C}} = \begin{pmatrix} m_T & -y_2 v \\ -y_1 v & -m_D \end{pmatrix}$$

$$\begin{pmatrix} T^0 \\ D_1^0 \\ D_2^0 \end{pmatrix} = \mathcal{N}\begin{pmatrix} \chi_1^0 \\ \chi_2^0 \\ \chi_3^0 \end{pmatrix}, \quad \begin{pmatrix} T^+ \\ D_2^+ \end{pmatrix} = \mathcal{C}_{\text{L}}\begin{pmatrix} \chi_1^+ \\ \chi_2^+ \end{pmatrix}, \quad \begin{pmatrix} T^- \\ D_1^- \end{pmatrix} = \mathcal{C}_{\text{R}}\begin{pmatrix} \chi_1^- \\ \chi_2^- \end{pmatrix}$$

Custodial symmetry limit $y_1 = y_2 \Rightarrow T = U = 0$ and $g_{Z\chi_1^0\chi_1^0} = 0$

$y_1 = y_2$ and $m_D < m_T \Rightarrow g_{h\chi_1^0\chi_1^0} = 0$

DTFDM: Fermion Masses and EW Oblique Parameters

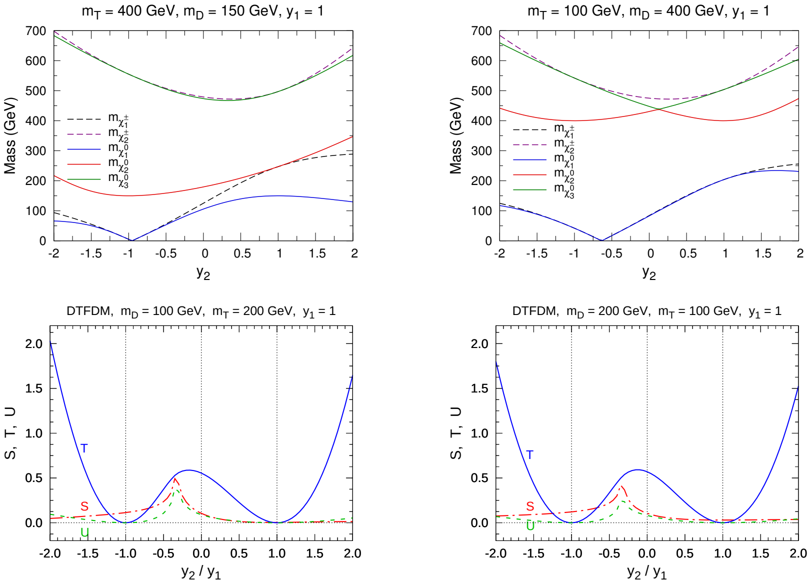

$y_1 = y_2 = 1$ (Custodial Symmetry)

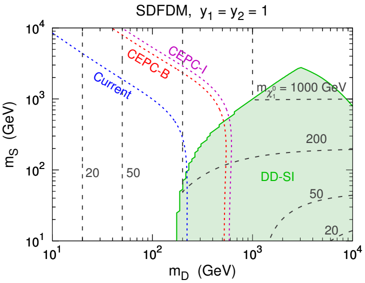

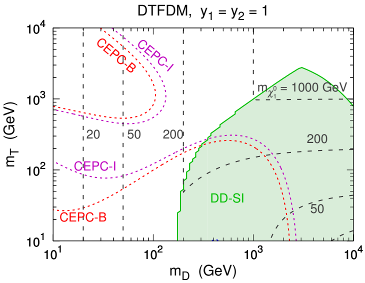

Dotted lines: expected 95% CL constraints from **current**, **CEPC-B**, and **CEPC-I** precisions of EW oblique parameters assuming $T = U = 0$

DD-SI: excluded by spin-independent direct detection at 90% CL

Dashed lines: DM particle mass

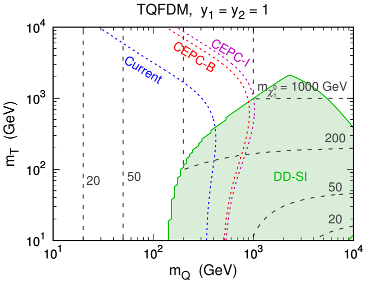

$y_1 = 1$ and $y_2 = 1.5$ (Custodial Symmetry Violation)

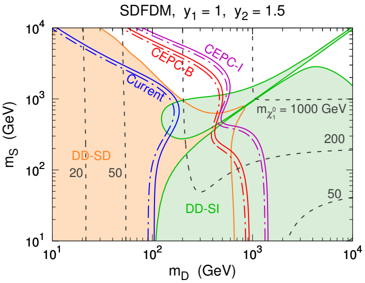

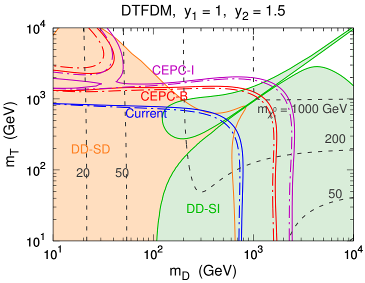

Expected 95% CL constraints from **current**, **CEPC-B**, and **CEPC-I** precisions of EW oblique parameters

Dot-dashed lines: free S, T, and U
Solid lines: assuming $U = 0$

DD-SI: excluded by SI direct detection
DD-SD: excluded by SD direct detection

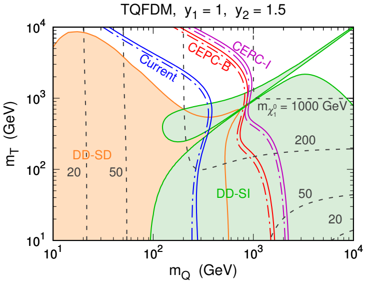

Singlet-Doublet Scalar Dark Matter (SDSDM)

A **real singlet scalar** $S \in (\mathbf{1}, 0)$ and a **complex doublet scalar** $\Phi \in (\mathbf{2}, 1/2)$:

$$\mathcal{L} \supset \frac{1}{2}(\partial_\mu S)^2 - \frac{1}{2} m_S^2 S^2 + (D_\mu \Phi)^\dagger D^\mu \Phi - m_D^2 |\Phi|^2 - (\kappa S \Phi^\dagger H + \text{h.c.}) - \frac{1}{2}\lambda_{Sh} S^2 |H|^2$$
$$-\lambda_1 |H|^2 |\Phi|^2 - [\lambda_2 (\Phi^\dagger H)^2 + \text{h.c.}] - \lambda_3 |\Phi^\dagger H|^2$$

- Custodial symmetry: (a) $\lambda_3 = 2\lambda_2$; b) $\lambda_3 = -2\lambda_2$ and $\kappa = 0$.
- The DM candidate can be either a **CP-even** or **CP-odd** scalar.

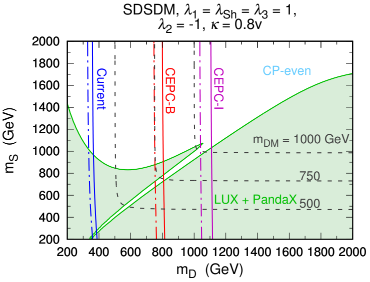

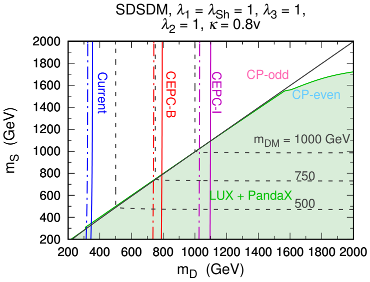

Dot-dashed lines: free S, T, and U **Solid lines:** assuming $U = 0$

Reduction to the Inert Higgs Doublet Model

In the limit $\kappa = 0$ and $m_S \to \infty$, the singlet decouples the SDSDM model reduces to the **inert Higgs doublet model** [Deshpande & Ma, PRD 18, 2574 (1978)]

- $\lambda_2 < 0$: **CP-even** DM candidate, coupling to the Higgs $\propto \lambda_1 + 2\lambda_2 + \lambda_3$
- $\lambda_2 > 0$: **CP-odd** DM candidate, coupling to the Higgs $\propto \lambda_1 - 2\lambda_2 + \lambda_3$
- $\lambda_3 > 2|\lambda_2|$: the DM candidate becomes **unstable** because the charged scalar in the dark sector is lighter

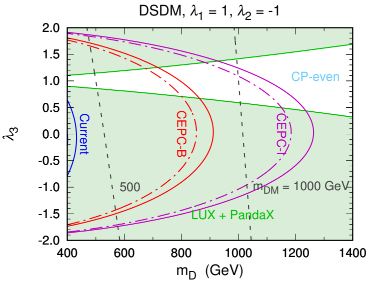

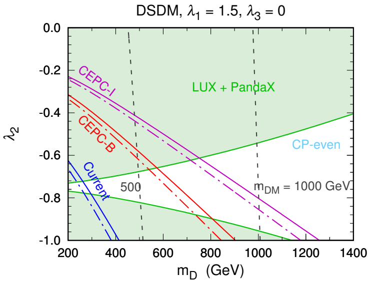

Dot-dashed lines: free S, T, and U **Solid lines:** assuming $U = 0$

Singlet-Triplet Scalar Dark Matter (STSDM)

A **real singlet scalar** $S \in (\mathbf{1}, 0)$ and a **complex triplet scalar** $\Delta \in (\mathbf{3}, 0)$:

$$-\mathcal{L} \supset \frac{1}{2} m_S^2 S^2 + m_\Delta^2 |\Delta|^2 + \frac{1}{2}\lambda_{Sh} S^2 |H|^2 + \lambda_0 |H|^2 |\Delta|^2 + \lambda_1 H_i^\dagger \Delta_j^i (\Delta^\dagger)_k^j H^k$$
$$+\lambda_2 H_i^\dagger (\Delta^\dagger)_j^i \Delta_k^j H^k - (\lambda_3 H_i^\dagger \Delta_j^i \Delta_k^j H^k + \lambda_3' |H|^2 \Delta_j^i \Delta_i^j + \lambda_4 S H_i^\dagger \Delta_j^i H^j + \text{h.c.})$$

- Define $\lambda_\pm \equiv \lambda_1 \pm \lambda_2$, and λ_3' and λ_0 can be absorbed into λ_3 and λ_+
- Custodial symmetry: $\lambda_- = \lambda_4 = 0$

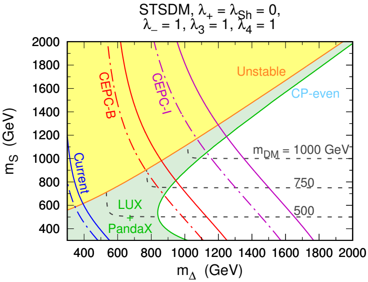

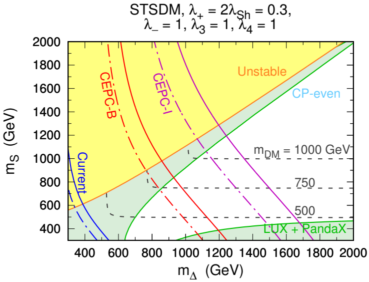

Dot-dashed lines: assuming $S = 0$ **Solid lines:** assuming $S = U = 0$

Quadruplet Scalar Dark Matter (QSDM)

A **complex quadruplet scalar** $X \in (\mathbf{4}, 1/2)$:

$$-\mathcal{L} \supset m_X^2 |X|^2 + \lambda_0 |H|^2 |X|^2 + \lambda_1 H_i^\dagger X_k^{ij} (X^\dagger)_{jl}^k H^l + \lambda_2 H_i^\dagger (X^\dagger)_{jk}^i X_l^{jk} H^l$$
$$-(\lambda_3 H_i^\dagger H_j^\dagger X_l^{ik} X_k^{jl} + \text{h.c.})$$

- Define $\lambda_\pm \equiv \lambda_1 \pm \lambda_2$, and λ_0 can be absorbed into λ_+ in the unitary gauge
- Custodial symmetry: $\lambda_- = \pm 2\lambda_3$

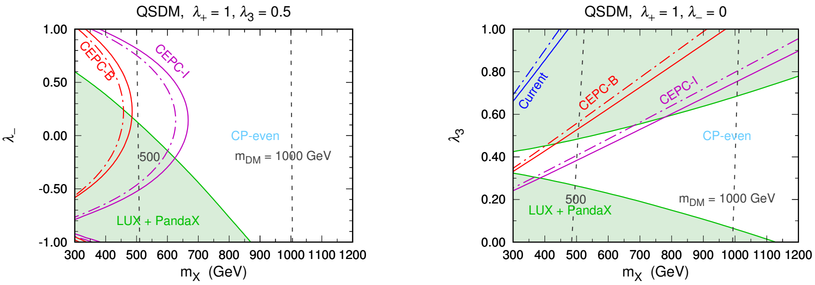

Dot-dashed lines: free S, T, and U **Solid lines:** assuming $U = 0$

Indirectly Probing Dark Matter via Higgs Measurements

Exploring Fermionic Dark Matter via Higgs Precision Measurements at the Circular Electron Positron Collider

Qian-Fei Xiang[1,2], Xiao-Jun Bi[1], Peng-Fei Yin[1], and Zhao-Huan Yu[3]

[1] *Key Laboratory of Particle Astrophysics, Institute of High Energy Physics, Chinese Academy of Sciences, Beijing 100049, China*

[2] *School of Physical Sciences, University of Chinese Academy of Sciences, Beijing 100049, China and*

[3] *ARC Centre of Excellence for Particle Physics at the Terascale, School of Physics, The University of Melbourne, Victoria 3010, Australia*

We study the impact of fermionic dark matter (DM) on projected Higgs precision measurements at the Circular Electron Positron Collider (CEPC), including the one-loop effects on the $e^+e^- \to Zh$ cross section and the Higgs boson diphoton decay, as well as the tree-level effects on the Higgs boson invisible decay. As illuminating examples, we discuss two UV-complete DM models, whose dark sector contains electroweak multiplets that interact with the Higgs boson via Yukawa couplings. The CEPC sensitivity to these models and current constraints from DM detection and collider experiments are investigated. We find that there exit some parameter regions where the Higgs measurements at the CEPC will be complementary to current DM searches.

[arXiv:1707.03094]

Higgs Precision Measurements at the CEPC

Table 3.9 Estimated precisions of Higgs boson measurements at the CEPC. All numbers refer to relative precisions except for m_H and BR($H \to$ inv), for which Δm_H and 95% CL upper limit are quoted respectively.

[CEPC-SPPC pre-CDR]

ΔM_H	Γ_H	$\sigma(ZH)$	$\sigma(\nu\bar{\nu}H) \times \mathrm{BR}(H \to b\bar{b})$
5.9 MeV	2.8%	0.51%	2.8%

Decay mode	$\sigma(ZH) \times \mathrm{BR}$	BR
$H \to b\bar{b}$	0.28%	0.57%
$H \to c\bar{c}$	2.2%	2.3%
$H \to gg$	1.6%	1.7%
$H \to \tau\tau$	1.2%	1.3%
$H \to WW$	1.5%	1.6%
$H \to ZZ$	4.3%	4.3%
$H \to \gamma\gamma$	9.0%	9.0%
$H \to \mu\mu$	17%	17%
$H \to \mathrm{inv}$	–	0.28%

CEPC will be a powerful **Higgs factory**; some of the precision measurements of the Higgs boson could be sensitive to DM models

$e^+e^- \to Zh$ Production in the SM

- The **Zh associated production $e^+e^- \to hZ$** is the primary Higgs production process at a 240 − 250 GeV Higgs factory
- For the measurement of the $e^+e^- \to hZ$ cross section, a **relative precision of 0.51%** is expected to be achieved at the CEPC with an integrated luminosity of 5 ab^{-1}

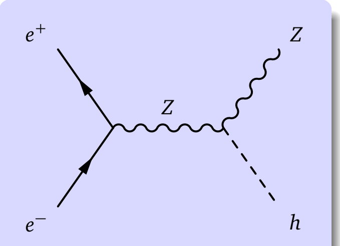

Tree level in the SM

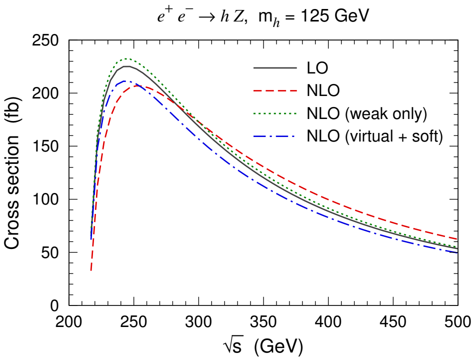

[Huang, Gu, Yin, ZHY, Zhang, arXiv:1511.03969, PRD]

Corrections to $e^+e^- \to Zh$ in the SDFDM Model

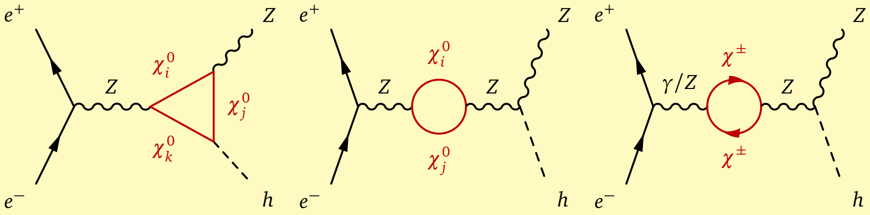

Vertex and propagator corrections at one-loop level

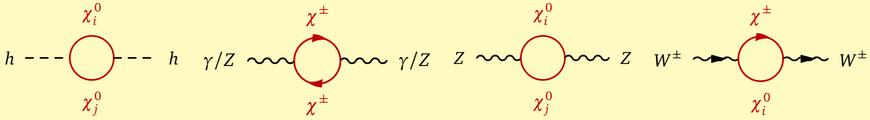

Self-energy corrections at one-loop level

Correction to the $e^+e^- \to Zh$ Cross Section

- Split the $e^+e^- \to Zh$ cross section into two parts: $\sigma = \sigma_0 + \sigma_{\rm BSM}$
- σ_0: SM prediction
- $\sigma_{\rm BSM}$: contribution due to physics beyond the SM
- When the dark sector fermions in the loops are able to close to their **mass shells**, the amplitudes would develop imaginary parts, and the contribution from the dark sector could vary dramatically

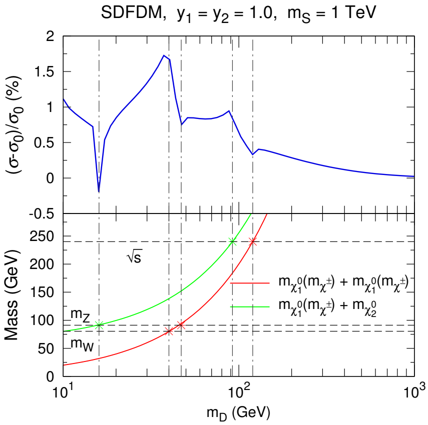

$\Rightarrow$ **Mass threshold effects** for $m_Z = m_{\chi_1^0} + m_{\chi_2^0}$, $m_W = m_{\chi_1^0} + m_{\chi^\pm}$, $m_Z = 2m_{\chi^\pm}$, and $\sqrt{s} = m_{\chi_1^0} + m_{\chi_2^0}$

Invisible Decays of the Z and Higgs Bosons

- If the kinematic conditions are satisfied, Z and h decays into a pair of DM particles would be allowed and **invisible**
- **LEP** experiments put an upper bound on the Z invisible decay width:
$$\Gamma_{Z,\mathrm{inv}}^{\mathrm{BSM}} < 2\ \mathrm{MeV} \text{ at } 95\%\ \mathrm{CL}$$
- The expected constraint on the h invisible decay width at the **CEPC** is
$$\Gamma_{h,\mathrm{inv}}^{\mathrm{BSM}} < 11.4\ \mathrm{keV} \text{ at } 95\%\ \mathrm{CL}$$

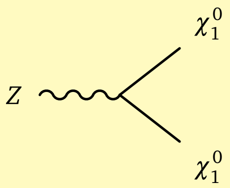

Z invisible decay

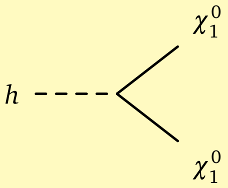

h invisible decay

SDFDM: CEPC Sensitivity and Current Constraints

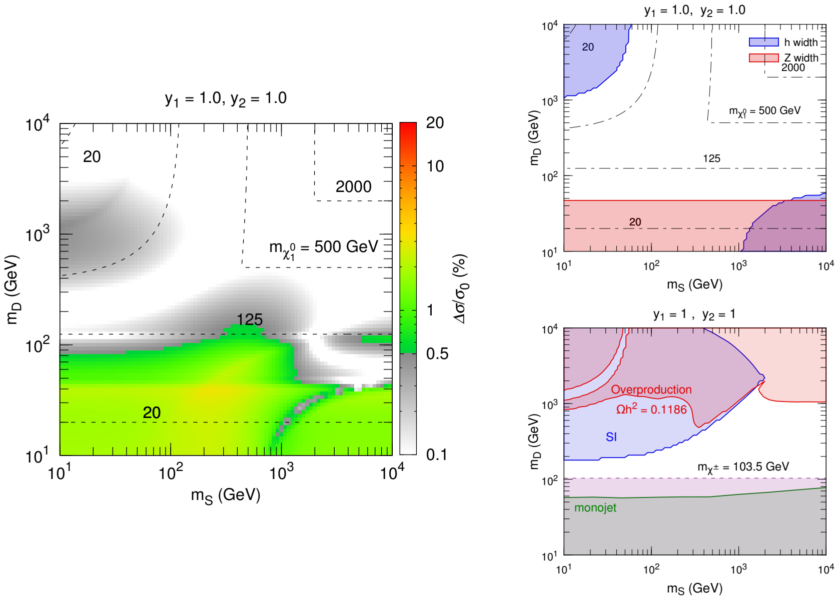

Extra Diagrams in the DTFDM Model

- In the **DTFDM model**, charged fermions $\chi_1^\pm$ and $\chi_2^\pm$ have both doublet and triplet components, allowing the existence of the $h\chi_i^\pm\chi_j^\pm$ couplings
- At one-loop level, the $h\chi_i^\pm\chi_j^\pm$ **couplings** give extra correction diagrams to $e^+e^- \to Zh$, and also give corrections to the $h \to \gamma\gamma$ **decay**
- **CEPC** is expected to measure the relative precision of the $h \to \gamma\gamma$ decay width down to 9.4%

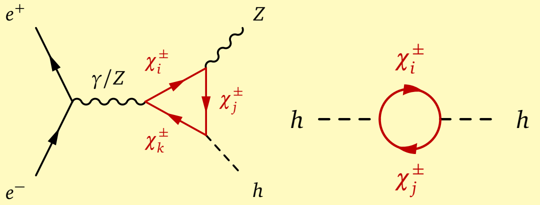

Extra corrections to $e^+e^- \to Zh$

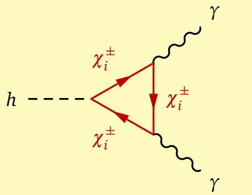

Corrections to $h \to \gamma\gamma$

DTFDM: CEPC Sensitivity and Current Constraints

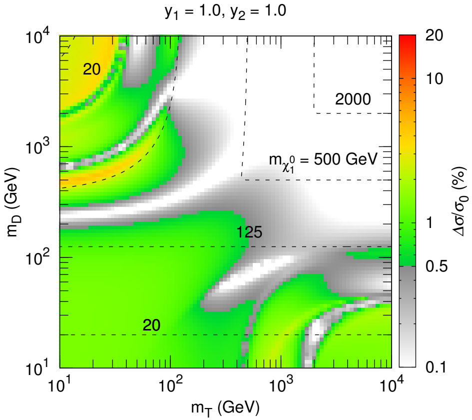

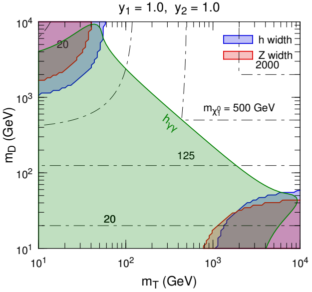

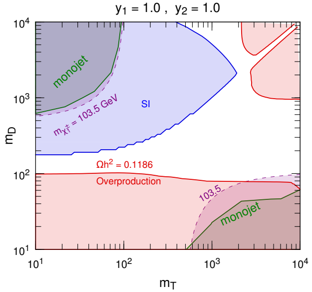

Homework

1. In the low velocity limit, derive the DM annihilation cross sections into 2γ, $\langle\sigma_{\rm ann}v\rangle$, in Page 8 from the effective operators $\mathcal{O}_F$ and $\mathcal{O}_S$; examine how the result would change if $\mathcal{O}_F$ is replaced by $\mathcal{O}'_F = \dfrac{1}{\Lambda^3}\bar{\chi}\chi F_{\mu\nu}F^{\mu\nu}$
2. Verify the expressions for $G_{\rm ZZ}$ and $G_{\rm AZ}$ in Page 16
3. In the low velocity limit, calculate the DM annihilation cross sections $\langle\sigma_{\rm ann}v\rangle$ into ZZ and e^+e^- for the effective operators $\mathcal{O}_{\rm F1}$, $\mathcal{O}_{\rm F2}$, and $\mathcal{O}_{\rm FH}$ in Page 16, and for $\mathcal{O}_{\rm FP}$ and $\mathcal{O}_{\rm FA}$ in Page 17
(Results can be found in arXiv:1404.6990)
4. For the SDFDM and TQFDM models in Page 40, derive the dark sector mass terms and mass matrices, whose forms should be similar to those given in Page 42 for the DTFDM model
(Results can be found in arXiv:1611.02186)
5. Draw all one-loop Feynman diagrams for the $h\to\gamma\gamma$ decay in the SM